Article

Metabolic Alteration Analysis of Steroid Hormones in Niemann–Pick Disease Type C Model Cell Using Liquid Chromatography/Tandem Mass Spectrometry

Ai Abe [1,2,†], Masamitsu Maekawa [1,2,*,†], Toshihiro Sato [2], Yu Sato [2], Masaki Kumondai [2], Hayato Takahashi [2], Masafumi Kikuchi [1,2], Katsumi Higaki [3], Jiro Ogura [2,‡] and Nariyasu Mano [1,2]

[1] Faculty of Pharmaceutical Sciences, Tohoku University, 1-1 Seiryo-machi, Aoba-ku, Sendai 980-8574, Japan; ai.abe.e8@tohoku.ac.jp (A.A.); masafumi.kikuchi.b2@tohoku.ac.jp (M.K.); mano@hosp.tohoku.ac.jp (N.M.)

[2] Department of Pharmaceutical Sciences, Tohoku University Hospital, 1-1 Seiryo-machi, Aoba-ku, Sendai 980-8574, Japan; toshihiro.sato@tohoku.ac.jp (T.S.); yu.sato.e7@tohoku.ac.jp (Y.S.); masaki.kumondai.d5@tohoku.ac.jp (M.K.); hayato.takahashi.e7@tohoku.ac.jp (H.T.); jiro.ogura@med.id.yamagata-u.ac.jp (J.O.)

[3] Division of Functional Genomics, Research Centre for Bioscience and Technology, Faculty of Medicine, Tottori University, 86 Nishi-cho, Yonago 683-8503, Japan; kh4060@tottori-u.ac.jp

* Correspondence: m-maekawa@tohoku.ac.jp; Tel.: +81-22-717-7541

† These authors contributed equally to this work.

‡ Current address: Graduate School of Pharmaceutical Sciences, Yamagata University, 2-2-2 Iida-nishi, Yamagata 990-9585, Japan.

Abstract: Niemann–Pick disease type C (NPC) is an autosomal recessive disease caused by a functional deficiency of cholesterol-transporting proteins in lysosomes, and exhibits various clinical symptoms. Since mitochondrial dysfunction in NPC has recently been reported, cholesterol catabolism to steroid hormones may consequently be impaired. In this study, we developed a comprehensive steroid hormone analysis method using liquid chromatography/tandem mass spectrometry (LC–MS/MS) and applied it to analyze changes in steroid hormone concentrations in NPC model cells. We investigated the analytical conditions for simultaneous LC–MS/MS analysis, which could be readily separated from each other and showed good reproducibility. The NPC phenotype was verified as an NPC model with mitochondrial abnormalities using filipin staining and organelle morphology observations. Steroid hormones in the cell suspension and cell culture medium were also analyzed. Steroid hormone analysis indicated that the levels of six steroid hormones were significantly decreased in the NPC model cell and culture medium compared to those in the wild-type cell and culture medium. These results indicate that some steroid hormones change during NPC pathophysiology and this change is accompanied by mitochondrial abnormalities.

Keywords: Niemann–Pick disease type C; steroid hormones; LC–MS/MS; mitochondria; ammonium solution; metabolic change

1. Introduction

Niemann–Pick disease type C (NPC) is an autosomal recessive disorder characterized by functional deficiencies affecting lysosomal cholesterol transport [1]. These deficits originate from a mutation in the *NPC1* [2,3] or *NPC2* genes [4,5], resulting in lipid accumulation [3,6] and the manifestation of various symptoms [1,7–9]. The main symptoms associated with the systemic and central nervous system include hepatosplenomegaly, cholestasis, lung lesions, epilepsy, cognitive dysfunction, and ataxia [10]. Neuropathologically, it is characterized by progressive degeneration of nerve cells, particularly cerebellar Purkinje cells, and foam macrophage infiltration [11]. NPC therapeutic agents, such as miglustat and 2-hydroxypropyl-β-cyclodextrin, have been developed, and although the use of miglustat has been approved in some countries [12], 2-hydroxypropyl-β-cyclodextrin is still

undergoing clinical trials [13]. Thus, despite various drug discovery approaches [14–17], clinical drug development has not yet been achieved. To date, the NPC pathology remains ambiguous, highlighting the necessity to explicate the associated underlying molecular mechanisms in an effort to overcome this disease.

Numerous studies have recently explored mitochondrial abnormalities in NPC. Briefly, these findings indicated that NPC-related lipid accumulation resulted in impaired autophagy, eventuating in abnormal mitochondrial activity [18–21]. Additionally, increased mitochondrial oxidative stress [22], downregulated ATP production [23], and reduced mitochondrial membrane potential have also been reported [24].

Steroid hormones are vital bioactive metabolites derived from cholesterol, and are synthesized in the endoplasmic reticulum and mitochondria [25–27]. These hormones are classified according to their function and structure as glucocorticoids, mineralocorticoids, estrogens, progestins, androgens, and neurosteroids [28,29].

Considering the mitochondrial abnormalities associated with NPC, an abnormal steroid hormone metabolism may be expected. Although some studies have reported an association between several steroid hormones and NPC [30–37], none have comprehensively analyzed the associated changes in steroid hormone metabolism. Therefore, analyzing metabolic changes in NPC may provide further understanding of NPC pathophysiology.

Although radio- and immunoassays are typically used in clinical laboratories to measure steroid hormone concentrations [38], they are limited by the occurrence of cross-reactivity and the inability to perform simultaneous analyses. Liquid chromatography–tandem mass spectrometry (LC–MS/MS) is a highly sensitive method utilized for comprehensive analyses [39] and would provide additional analytical benefits since the amount of steroid hormones in cells or body fluids are very small. Furthermore, although many LC–MS/MS techniques combined with derivatization have been reported [40,41], they are often unsuitable for the comprehensive analysis of steroid hormones, which possess a variety of functional groups.

In this study, we aimed to analyze the metabolic alterations of steroid hormones in NPC and develop a simultaneous steroid hormone analysis method using LC–MS/MS, thereby allowing for a deeper understanding of the NPC pathophysiology and its involvement in mitochondrial steroid hormone production. A gonad-derived NPC cell model was used in this study [42]. First, simultaneous analysis conditions were developed for 13 steroid hormones (Figure 1). ESI–MS/MS, LC, and pretreatment conditions were investigated and the analytical method was validated. Next, we verified the characteristics and morphology of NPC model cells. Finally, we analyzed the NPC model and wild-type cells and compared their steroid hormone levels.
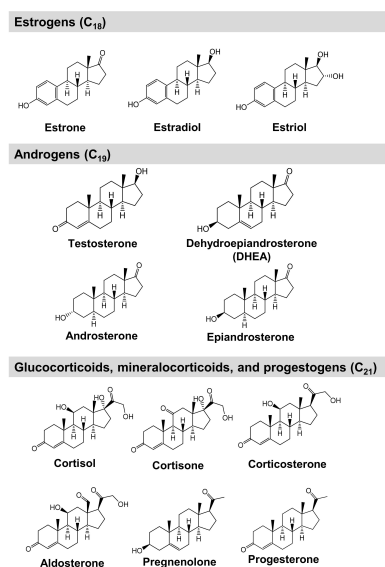

Figure 1. Chemical structures of steroid hormones analyzed in this study.

2. Results and Discussion

2.1. MS/MS Optimization for Steroid Hormone Analysis

LC–MS/MS is capable of simultaneous steroid hormone analyses, thus providing a suitable platform for the development of a comprehensive protocol targeted for these hormone concentrations [39–41,43–49]. Although derivatization by conjugating proton affinity groups to analytes is widely utilized [40,41,43–48], LC–MS/MS analysis methods without derivatization have recently been reported [49–51]. Moreover, Li et al. and Gaudl et al. utilized ammonium fluoride as an additive, thereby allowing for the simultaneous analysis of various estrogens [49,51]. Considering this, the current study was aimed at developing a comprehensive steroid hormone-specific analytical method using LC–MS/MS without derivatization. MS parameters that were optimized via the infusion of standard solutions included declustering potential (DP), collision energy (CE), and cell exit potential (CXP). The MS polarity was separated into positive and negative ion detection modes in a similar manner as described in previous reports [50,51]. A total of ten and three compounds were observed in positive and negative ion detection modes, respectively (Table 1). These base peaks subsequently served as precursor ions, and the most intense selected reaction monitoring (SRM) transitions and CE values were optimized accordingly and are presented in Table 1.

Table 1. SRM parameters and LC retention times for steroid hormones.

Analytes	Q1 (*m/z*)	Precursor Ion Form	Q3 (*m/z*)	DP (V)	CE (V)	CXP (V)	EP (V)	Polarity	Retention Time (min)
Testosterone	289.0	$[M + H]^+$	97.1	100	8	29	6	Positive	7.1
Androsterone	273.1	$[M - H_2O + H]^+$	255.1	146	8	19	14	Positive	10.1
Epiandrosterone	273.2	$[M - H_2O + H]^+$	255.2	146	8	19	14	Positive	8.4
DHEA	271.0	$[M - H_2O + H]^+$	253.1	81	12	19	4	Positive	7.8
Cortisol	363.0	$[M + H]^+$	120.9	100	8	31	8	Positive	4.1
Cortisone	361.1	$[M + H]^+$	163.0	100	8	33	10	Positive	3.9
Corticosterone	347.2	$[M + H]^+$	329.0	101	6	21	16	Positive	5.6
Aldosterone	361.1	$[M + H]^+$	343.1	61	8	25	6	Positive	3.3
Pregnenolone	299.2	$[M - H_2O + H]^+$	91.1	161	8	71	8	Positive	10.6
Progesterone	315.0	$[M + H]^+$	97.0	100	8	27	6	Positive	10.3
Estrone	269.0	$[M - H]^-$	144.8	−80	−6	−48	−9	Negative	6.4
Estradiol	271.0	$[M - H]^-$	182.9	−100	−15	−58	−11	Negative	6.1
Estriol	287.1	$[M - H]^-$	170.8	−140	−15	−50	−11	Negative	3.0
Testosterone-$^2H_3$	292.1	$[M + H]^+$	96.9	100	8	27	6	Positive	7.1
Androsterone-$^2H_4$	277.2	$[M - H_2O + H]^+$	259.1	121	8	19	14	Positive	10.0
DHEA-$^2H_6$	276.9	$[M - H_2O + H]^+$	259.0	211	12	25	11	Positive	7.8
Cortisol-$^{13}C_3$	366.2	$[M + H]^+$	123.9	101	8	31	8	Positive	4.1
Aldosterone-$^2H_7$	368.3	$[M + H]^+$	350.0	91	8	25	16	Positive	3.3
Pregnenolone-$^{13}C_2,^2H_2$	303.2	$[M - H_2O + H]^+$	91.1	161	8	71	8	Positive	10.6
Progesterone-$^2H_9$	324.2	$[M + H]^+$	100.1	100	8	29	8	Positive	10.2
Estrone-$^2H_4$	273.0	$[M - H]^-$	146.9	−80	−6	−52	−11	Negative	6.4
Estradiol-$^{13}C_3$	274.2	$[M - H]^-$	186.0	−100	−15	−56	−9	Negative	6.1
Estriol-$^{13}C_3$	290.0	$[M - H]^-$	173.9	−140	−15	−50	−11	Negative	3.0

Mobile phase additives, such as ammonium solutions [52–54], were investigated in the negative ion detection mode to increase analysis sensitivity. The aqueous ammonium solution exhibited the most intense peaks (Figure 2). Considering that the pH of the ammonium aqueous solution [52–54] and ammonium fluoride solution [49,51] is approximately 11 and the pKa of the phenolic groups on estrogens is approximately 10.8 [55], these solutions negatively ionize more phenolic groups, thereby producing stronger ion intensities than neutral or acidic pH solutions.
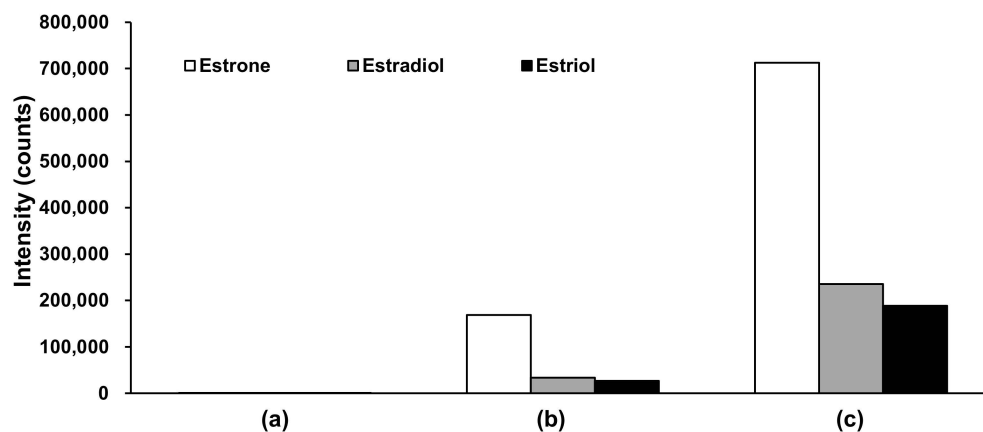
Figure 2. Comparison of peak intensities in negative ion detection mode for various mobile phases. (**a**) Acidic conditions using mobile phase A: Formic acid/water (0.1:100, *v/v*) and mobile phase B: Formic acid/MeOH/ACN (0.1:50:50, *v/v/v*); (**b**) weak basic conditions using mobile phase A: Formic acid/water (0.1:100, *v/v*) and mobile phase B: 1 M ammonium acetate aqueous solution/MeOH/ACN (0.1:50:50, *v/v/v*); (**c**) basic conditions using mobile phase A: 28% ammonium aqueous solution/water (0.1:100, *v/v*) and mobile phase B: 28% aqueous ammonium solution/MeOH/ACN (0.1:50:50, *v/v/v*). ACN, acetonitrile; MeOH, methanol.

2.2. LC optimization for Steroid Hormone Analysis

Since the structural isomers in this study exhibited similar SRM transitions, we investigated the LC conditions for isomer separation. Reversed-phase chromatography is the most suitable method for LC separation of steroid hormones. Various stationary phase columns, such as phenyl-hexyl [50], poly[styrenevinylbenzene] particle (POROS™ column) [51], and octadecylsilyl (ODS) columns have previously been used [49,56]. The ODS-bonded column was utilized in the current study, considering that it allows good retention of steroid hormones. Furthermore, two simultaneous LC–MS/MS analysis conditions were examined and developed in the current study; one for the positive and the other for the negative ion detection modes.

An ODS-bonded core-shell silica gel was used as the analytical column for LC separation and subsequent detection of analytes in the positive ion detection mode, and formic acid was used as an additive under acidic conditions. Several gradient conditions were investigated and revealed that good separation was achieved when the mobile phase B concentration increased from 35% to 80% (Figure 3a). The associated retention times are listed in Table 1.
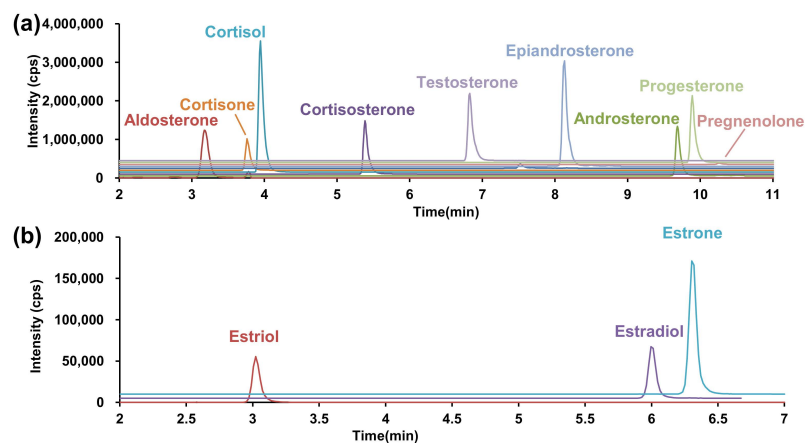

Figure 3. SRM chromatogram under optimized conditions. (**a**) Positive ion detection mode, (**b**) negative ion detection mode. SRM, selected reaction monitoring.

Next, the LC conditions were optimized for the negative ion detection. A highly sensitive analysis was performed at pH 11 using an aqueous ammonium solution as an additive for MS–MS optimization. However, considering that silica particles of silanol group are disrupted under basic conditions, general ODS-bonded silica columns cannot be used. Therefore, we utilized a Triart C18 Plus, an ethylene crosslinked-hybrid silica gel column in which the basicity and pressure resistance of the silica gel were improved. The LC gradient separation conditions required for separating estrone and estradiol, while retaining the estriol, were evaluated. Good LC separation was achieved when the mobile phase B concentration increased from 40% to 75% in 7 min (Figure 3b).

2.3. Extract Recovery

Pretreatment, such as solid-phase extraction [49–51] and liquid–liquid extraction [45,47,48,56], is imperative when analyzing endogenous compounds in biological samples. Although solid-phase extraction is a simple sample pretreatment method, the required solid-phase cartridges are expensive. Contrarily, liquid–liquid extraction allows for effortless removal of contaminants using two immiscible liquids. Considering that all analytes and ISs are non-ionized steroids, the latter extraction method can be easily applied in the context of this study. As such, ethyl acetate (AcOEt) and tert-butyl methyl ether (tBME) were used as the organic layer while water was used as the aqueous layer. Furthermore, five combinations of organic solvents were investigated and the absolute recovery rate was used for performance evaluation. The latter evaluation revealed that highly stable recovery of steroid hormones was achieved on performing liquid–liquid extraction twice with AcOEt (Table S1).

2.4. Analytical Method Validation

To effectively quantify metabolites in a biological sample, it is important to ensure good reliability of the analytical method. Therefore, validation of the developed method is required to confirm the validity and reliability of the process. In this section, we verify the matrix effect, calibration curve linearity, and reproducibility to evaluate the reliability of the analysis method by using cells and media. In the analysis of endogenous substances, it is difficult to obtain a blank matrix without utilizing steroids. As such, the validity of this analytical method was evaluated based on previous reports [57–61].

2.4.1. Matrix Factor

The matrix effect of the analytical method, which was evaluated for each matrix of the cells and medium, is a combination of the recovery rate and extraction process efficiency. Matrix factor (MF) [57,58,62] and the IS-normalized MF were calculated to evaluate the matrix effect [57,58,62]. Several MFs were approximately $100 \pm 15\%$ in both the cells and medium (Table S2A). Although some analytes showed >15% matrix effects (epiandrosterone on medium and estrone, estradiol, estriol, estrone-$^2H_4$, estradiol-$^{13}C_3$, and estriol-$^{13}C_3$ in cells), their MFs were normalized within $100 \pm 15\%$ using their ISs (Table S2B). In other words, the matrix effect on the quantification of all analytes was compensated for by their ISs.

2.4.2. Calibration Curves

Calibration curves were constructed for the quantification of steroid hormones. Considering that the analytical methods were unaffected by the matrix, as discussed in Section 2.4.1, water was used as a surrogate matrix that did not include the analytes. Calibration curves were prepared using each IS, all of which showed good linearity (Table S3).

2.4.3. Reproducibility Test

Quality control (QC) samples, which were prepared by spiking the matrix with standard solutions, were quantified using calibration curves. The accuracy and precision of the method was evaluated by using the relative error (RE) and the coefficient of variation (CV), respectively. Considering the low analyte concentrations present in the matrix, the

calculations were performed to accommodate their endogenous amounts. Thus, accuracy was evaluated based on the spiked QC samples. In the cell samples, aldosterone, androsterone, and epiandrosterone levels were $>\pm15\%$ (Table S4A,C) and estrogen levels were within $\pm15\%$ in all assays (Table S4B,D). In the medium samples, aldosterone, testosterone, androsterone, and epiandrosterone levels were $>\pm15\%$ (Table S5A,C) and estrogen levels were within $\pm15\%$ in all assays (Table S5B,D). An important consideration is that, for analytes presenting with larger errors, LC–MS/MS-calculated steroid hormone concentrations may differ from their actual values.

2.5. Cells

Because steroid hormones exhibit sex-related differences in their expression and diurnal changes, NPC model cells were used to analyze the metabolic changes associated with steroid metabolism in NPC pathology. Two causative genes, namely *NPC1* and *NPC2*, are mutated in patients with NPC [1,7,9,63]. Considering that 95% of NPC cases present with mutation in the *NPC1* gene [1,7,9,64], the *NPC1* mutant cell is often used as an NPC model cell [42,64]. In this study, we used an *Npc1*-deficient Chinese hamster ovary (CHO) cell line established using gene trap mutagenesis as an NPC model cell [42]. The characteristics of the NPC model cells were verified before LC–MS/MS analysis.

2.5.1. Confirmation of Cholesterol Accumulation Using Filipin Staining

Since NPC patients lack functional cholesterol-transporting proteins [1,6], lysosomal cholesterol accumulates in cells [65–67]. Therefore, we confirmed unesterified cholesterol accumulation in NPC model cells (Figure S1) using filipin staining [65–68], which is a standard and conclusive diagnostic method for NPC [7,9]. As such, it was confirmed that the model cells used here successfully represented NPC.

2.5.2. Organelle Observation

Organelle morphology of the NPC model cells was confirmed via staining with Organelle-ID-RGB, a mixed reagent containing three fluorescent compounds for mitochondria, nuclei, and lysosomes. The fluorescence signal for mitochondrial morphology (green) indicated that the wild-type cells were rod-shaped (Figure S2A). In agreement with previous reports [18,20], numerous spherical mitochondria were observed in the NPC model cells and fragmentation was also confirmed (Figure S2B). In addition, lysosome (red) and mitochondria (green) localization were observed to be complementary (Figure S3D). In other words, the mitochondria were involved in the lysosomal degradation process and presented incomplete mitochondrial morphology associated with NPC, which is consistent with previous reports [20,69,70].

2.6. Steroid Hormone Analysis in NPC Model Cell

Finally, steroid hormones in the NPC cells and the medium were analyzed, and the associated metabolic changes were investigated. The cell culture and sample collection scheme is summarized in Figure S3. Studies on the in vitro metabolism of steroid hormones have often used media as samples [71,72]. Considering that phenol red has estrogen-like action [73,74], the current study utilized medium that excluded phenol red. In addition, fetal bovine serum (FBS) acts as a nutrient and contains steroid hormones. As such, and based on previous reports [75,76], the 10% FBS-supplemented medium was replaced with FBS-free medium in the current study. Furthermore, both medium [77–83] and cells [84] have previously been used as samples. Following analysis, it was observed that testosterone, androsterone, progesterone, and estrone levels were significantly decreased in the NPC model cells (Figure 4 and Table S6). Moreover, testosterone levels were particularly increased in the NPC model compared to the wild-type cells, while androsterone levels were significantly decreased in the NPC cells.
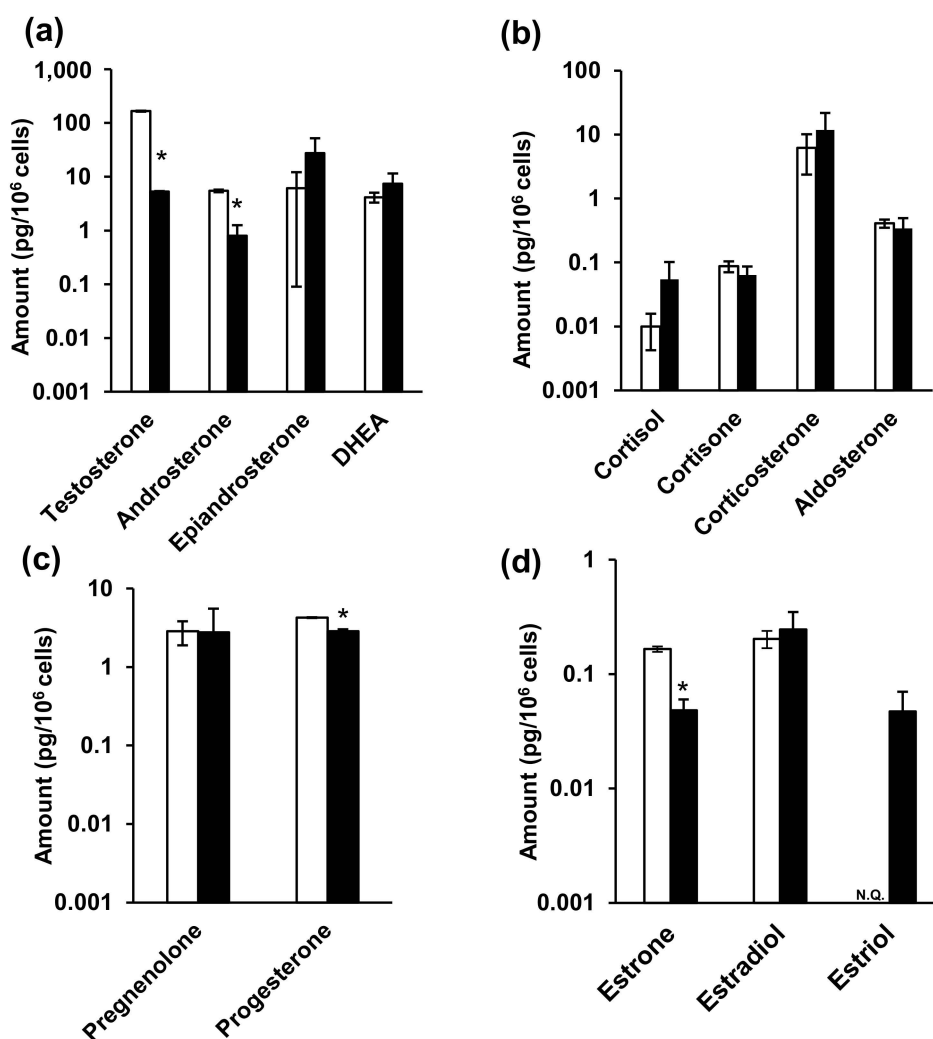
Figure 4. The amounts of steroid hormones in the cells. (**a**) Androgens, (**b**) glucocorticoids and mineralocorticoid, (**c**) progestins, and (**d**) estrogens. White and black bars indicate wild-type and NPC model cells, respectively. * indicates significant differences observed using Wilcoxon's test ($p < 0.05$). NPC, Niemann–Pick disease type C; N.Q., not quantified.

In contrast, epiandrosterone, dehydroepiandrosterone (DHEA), glucocorticoid, and aldosterone levels were not significantly different between two cells. Furthermore, progesterone levels significantly decreased in NPC cells (wild-type: 4.27 ± 2.87 pg/10^6 cells, NPC model cells: 0.342 ± 0.148 pg/10^6 cells), while pregnenolone levels did not change. Among the estrogens, estrone levels significantly decreased in NPC cells (wild-type: 0.166 ± 0.00918 pg/106 cells, NPC model cells: 0.0483 ± 0.0120 pg/106 cells), estradiol levels were not significantly different, and estriol was only detectable in the NPC model cells, in comparison to their levels in the wild-type cells.

Medium analysis indicated the presence of steroid hormones, even in FBS-free medium without cell cultures. Therefore, we analyzed both fresh and 48 h cell culture media and subsequently calculated the difference in steroid hormone levels between the two media. A sub-zero (negative) difference in epiandrosterone and corticosterone levels (Figure 5 and Table S5) indicated that the steroid hormone levels were decreased in the 48 h cell culture medium compared to those in fresh medium. This may have resulted from the chemical conversion of steroid hormones into the medium or, alternatively, their cellular uptake. Steroid hormones are generally chemically stable [85,86], and FBS-free medium contains no metabolic enzymes, suggesting that cellular uptake was the cause. Steroid hormones are passively taken up by cells, not via transporters. Considering that intracellu-

lar epiandrosterone and corticosterone concentrations were higher than those of the other hormones (Figure 4 and Table S4), their uptake may be greater than that of the other steroid hormones. Among the corticosteroids, cortisone levels decreased significantly in NPC model cell, whereas those of the others did not change. Furthermore, progesterone levels decreased significantly among progestins. Among the estrogens, estrone and estradiol levels were significantly decreased. Lastly, estriol, androsterone, and pregnenolone were not detected in the culture media.
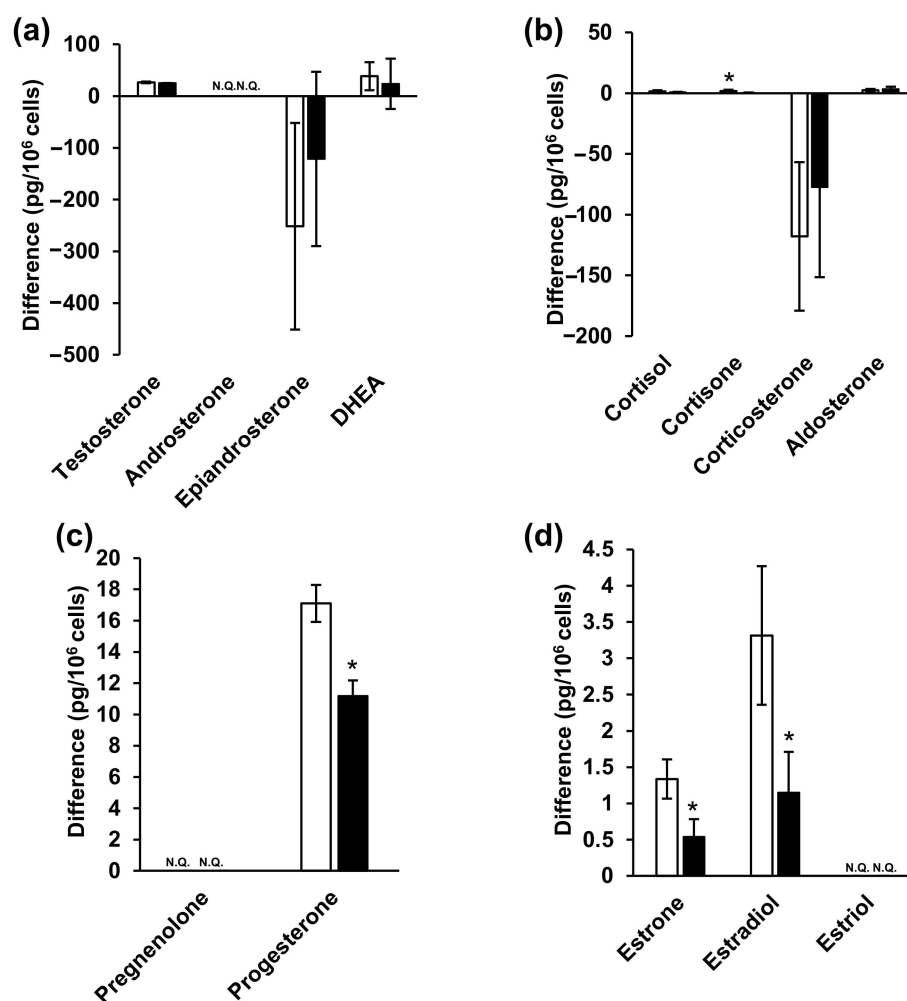

Figure 5. Steroid hormone concentrations in the medium. (**a**) Androgens, (**b**) glucocorticoids and mineralocorticoid, (**c**) progestins, (**d**) estrogens. White and black bars indicate wild-type and NPC model cells, respectively. * indicates significant differences observed using Wilcoxon's test ($p < 0.05$). NPC, Niemann–Pick disease type C; N.Q., not quantified.

In summary, the results of steroid hormone analyses in cells and media indicated that testosterone, androsterone (classified as androgens), progesterone (progestins), as well as estrone and estradiol (classified as estrogens) decreased significantly (Figures 4 and 5, Tables S4 and S5). Steroid hormones can be synthesized from both mevalonic acid and exogenous cholesterol [87], explaining their detection even in patients with abetal-ipoproteinemia [88]. Steroid hormones are synthesized in specific organs, including the adrenal cortex, gonads, and brain [26,36,89]. First, unesterified cholesterol is absorbed into the mitochondria by steroid-producing acute regulatory protein (StAR) [90]. CYP-scc subsequently produces pregnenolone [91], which is sequentially metabolized via two mechanisms. The first mechanism involves 3β-hydroxy group oxidation, catalyzed by 3β-hydroxysteroid dehydrogenase (3β-HSD) [92], to produce progesterone. Additionally,

3β-HSD 2 is expressed in ovaries. The second mechanism involves side-chain cleavage with 17α-hydroxylase/17,20 lyase (CYP 17) [93], which produces DHEA [94]. Interestingly, CYP 17 is also expressed in the ovaries [95]. Progesterone is metabolized to deoxycorticosterone [96], which is further metabolized, along with 11-deoxycortisol, by 11β-hydroxylase (CYP11B1) in mitochondria [26]. Corticosterone is then metabolized to aldosterone by aldosterone synthase (CYP11B2) [26]. Moreover, 11-deoxycortisol is metabolized to cortisol and cortisone while aldosterone and cortisol are also produced in the adrenal cortex. In this study, ovarian cells were used. These cells do not generate aldosterone, cortisol, or cortisone; however, these hormones were detected in these cells (Figures 4 and 5, Tables S4 and S5). It is possible that the duration of cell culture in FBS-free medium might have been insufficient. DHEA and androstenedione are metabolized to androstenediol and testosterone, respectively, by 17β-HSD [97], and 17β-HSD 2 is expressed in the ovaries [98]. Androstendiol is metabolized to testosterone by 3β-HSD, and androstenedione and testosterone are metabolized to estrone and estradiol, respectively, by aromatase (CYP19A). Estriol is produced from 16-hydroxyestrone by both P450 and 17β-HSD [99]. Aromatase, 3β-HSD, and 17β-HSD were expressed in cells used in this study.

We found decreased levels of various steroid hormones (Figures 4 and 5, Tables S4 and S5), suggesting that steroid hormone production may be lower in NPC cells than in normal cells. Most steroidogenic enzymes are in the mitochondria or endoplasmic reticulum and some use coenzymes [27]. NAD, for example, is the coenzyme of 3β-HSD, and is generally used for mitochondrial energy production [92,100]. Although both mitochondrial membrane potential and ATP synthesis must be fully functional for the synthesis of steroid hormones [101,102], mitochondrial dysfunction due to NPC pathology was observed in this study (Figure S2). Similarly, patients with early diabetes present with reduced levels of some neurosteroids and neurosteroid-producing enzymes in the brain in addition to mitochondrial dysfunction [103–105]. Glucocorticoid levels decrease in nicotinamide nucleotide transhydrogenase (NNT) deficiency [106]. NNT uses transmembrane potential to regenerate NADPH and the mitochondrial antioxidant system to regulate energy metabolism. Therefore, NNT deficiency impairs steroid hormone synthesis by reducing the energy supply [106]. As such, it may be concluded that steroid hormone production is impaired in patients with mitochondrial disorders (Figure 6).
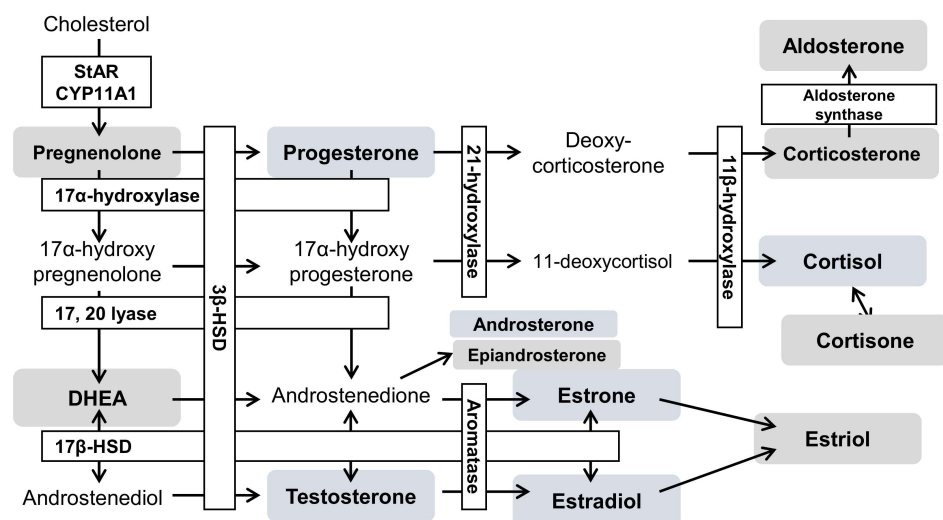

Figure 6. The hypothesis of an altered steroid hormone metabolism in NPC. Blue boxes indicate a decrease; gray boxes indicate no change. The open text indicates the absence of analytes in this study. CYP11A1, cytochrome P450 family 11 subfamily A member 1; 3β-HSD, 3β-hydroxysteroid dehydrogenase; 17β-HSD, 17β-hydroxysteroid dehydrogenase; CYP11B1, 11β-hydroxylase; CYP11B2, aldosterone synthase; CYP17A, 17α-hydroxylase/17,20 lyase; CYP19A, aromatase; CYP21A, 21-hydroxylase; DHEA, dehydroepiandrosterone; StAR, steroidogenic acute regulatory protein.

In summary, NPC may involve multiple mitochondrial disorders and the reduction of various steroid hormones. Generally, steroid hormones are secreted into the blood and exert their effects via various nuclear receptors [28,107–109]. Estrogens, progesterone, and androgens, also known as sex hormones, are involved in the maintenance of cognitive and reproductive function. Furthermore, neurosteroids, which are synthesized in the brain, affect neuronal growth, survival, and differentiation, [110–112] and have neuroprotective effects [110], while some neurosteroids act as neurotransmitters [113]. Purkinje cells are the major neurosteroid production sites, and mammals actively synthesize neurosteroids from cholesterol [114]. However, cerebellar Purkinje neurons die in NPC patients [115]. Although the brain and neurosteroidogenic functions in NPC are unknown, they should be analyzed in the future.

Patients with NPC present with various symptoms, including inflammation and neurological symptoms [1,7,9,116]. Additionally, neurosteroid production may be affected by Purkinje cell degeneration [115]. In the future, we aim to analyze steroid hormones in humans and clarify their effects on NPC pathology.

3. Materials and Methods

3.1. Chemicals and Reagents

Cortisol and testosterone-[^{2}H$_3$] were purchased from Sigma-Aldrich (St. Louis, MO, USA). Cortisone, aldosterone, corticosterone, and progesterone were purchased from Steraloids (Newport, RI, USA) and pregnenolone was purchased from Funakoshi (Tokyo, Japan). Dehydroepiandrosterone, epiandrosterone, and androsterone were obtained from Tokyo Chemical Industry Co., Ltd., (Tokyo, Japan). Estrone, estradiol, estriol, acetic acid (special grade reagent), tBME, and filipin complex were purchased from Nacalai Tesque (Kyoto, Japan). Progesterone-[^{2}H$_9$], 17β-estradiol-[^{13}C$_3$], aldosterone-[^{2}H$_7$], and estrone-[^{2}H$_4$] were acquired from ISOTEC (Miamisburg, OH, USA). Cortisol-[^{13}C$_3$], androsterone-[^{2}H$_4$], estriol-[^{13}C$_3$], dehydroepiandrosterone-[^{2}H$_6$], and pregnenolone-[^{13}C$_2$,^{2}H$_2$] were purchased from Cambridge Isotope Laboratories (Tewksbury, MA, USA). Testosterone, formic acid (special grade reagent), 28% aqueous ammonia solution (special grade), and the wako free cholesterol E-test were obtained from Fuji Film Wako Pure Chemical Industries (Osaka, Japan). First-grade methanol and AcOEt were first distilled following their purchase from Fuji Film Wako Pure Chemical Industries (Osaka, Japan). HPLC-grade acetonitrile was obtained from Kanto Chemical Co., Inc. (Tokyo, Japan). Ultrapure water was purified using a Puric-α purification system (ORGANO CORPORATION, Tokyo, Japan). In addition, Organelle-ID-RGB® Reagent I was acquired from Enzo Life Sciences Inc. (Farmingdale, NY, USA).

3.2. LC–MS/MS Equipment

A QTRAP 6500 linear ion trap-quadrupole hybrid tandem mass spectrometer (SCIEX, Framingham, MA, USA) equipped with an ESI probe was connected to a Nexera series ultra-high-performance liquid chromatograph (Shimadzu, Kyoto, Japan). Measurements were performed in positive or negative ion detection modes, while quantitative analysis was performed via measurement and peak processing using Analyst 1.6.2 and SCIEX OS-Q (SCIEX).

3.3. ESI–MS/MS Conditions

In both the positive and negative ion detection modes, 1 μg/mL of each standard solution was infused at a flow rate of 10 μL/min, while the mobile phases A and B were delivered at a flow rate of 390 μL/min and a ratio of 2:3. Optimization of each SRM condition was established by analyte diluting with the mobile phases, and the optimizations are listed in Table 1. Additionally, the optimized ion source parameters used in each mode are listed in Table S8.

3.4. LC Conditions

3.4.1. Positive Ion Detection Mode

Gradually changing ratios of formic acid/water (0.1:100, *v/v*) and formic acid/methanol/acetonitrile (0.1:50:50, *v/v/v*) served as mobile phases A and B, respectively (Table S9A). A flow rate of 0.4 mL/min was applied in a CAPCELL CORE C18 column (2.1 mm inner diameter × 150 mm, 2.7 μm; Osaka Soda; Osaka, Japan) set at 40 °C. A sample volume of 50 μL was injected into the LC–MS/MS system for analysis.

3.4.2. Negative Ion Detection Mode

Mobile phases A and B were comprised of 28% aqueous ammonia/water (0.1:100, *v/v*) and 28% aqueous ammonia/methanol/acetonitrile (0.1:50:50, *v/v/v*), respectively, and were delivered in gradient mode at a flow rate of 0.4 mL/min. Triart C18 Plus (2.1 mm inner diameter × 150 mm, 3 μm; YMC; Kyoto, Japan) was utilized at a temperature of 40 °C. A sample volume of 50 μL was injected, and the obtained gradient conditions are listed in Table S9B.

3.5. Preparation of Standard Steroid Hormone Solutions

The standard reagents were precisely weighed for each steroid hormone and subsequently dissolved in ethanol, obtaining a concentration of approximately 100 μg/mL. Each standard stock solution was mixed and diluted with ethanol and subsequently utilized for calibration curve construction and QC purposes. The standard solution for the calibration curve was prepared in the range of 1 pg/mL to 100 ng/mL (detailed in Section 3.9). The standard solutions utilized for QC purposes during positive ion detection included QCL (0.6 ng/mL), QCM (6 ng/mL), and QCH (50 ng/mL), while those for negative ion detection included QCL (0.06 ng/mL), QCM (0.6 ng/mL), and QCH (50 ng/mL). All standards were stored at −20 °C.

3.6. Preparation of IS Solution

Compounds labeled with stable isotopes were precisely weighed and dissolved in ethanol to obtain a concentration of 10 μg/mL. Each standard solution was further diluted with ethanol to prepare a 2 ng/mL mixed solution. Subsequently, each standard stock solution was diluted with AcOEt to prepare a mixed IS solution. The 17β-estradiol-[$^{13}C_3$], aldosterone-[$^2H_7$], estrone-[$^2H_4$], progesterone-[$^2H_9$], cortisol-[$^{13}C_3$], and estriol-[$^{13}C_3$] solutions were diluted to 30 pg/mL, whereas the androsterone-[$^2H_4$], dehydroepiandrosterone-[$^2H_6$], and pregnenolone-[$^{13}C_2,^2H_2$] solutions were diluted to 300 pg/mL. All prepared standards were stored at −20 °C.

3.7. Liquid–Liquid Extraction

Following addition of 1 mL IS solution diluted in AcOEt and 3 mL AcOEt to 2 mL of sample solution (medium or cell suspension), the mixtures were centrifuged at 3000× *g* for 10 min, and the separated upper layer was transferred to another tube. Centrifugation was repeated following addition of 4 mL AcOEt to the lower layer, and the resulting upper layer was extracted again. The upper layers obtained using the two liquid–liquid extractions were combined, evaporated under a nitrogen stream, and re-dissolved in 100 μL water/methanol (50:50, *v/v*). Of these prepared samples, 50 μL aliquots were injected for analysis in both the positive and negative ion detection modes.

3.8. Matrix Effect

To evaluate the matrix effect, MF and IS-normalized MF was determined following the introduction of standards to the matrix using the calculations depicted below [57,60,61,117]. Briefly, 2 mL of cell suspension containing 8.6 × 10^6 cells or medium was used as the matrix, and 100 μL of 2 ng/mL standard solution and 100 μL of 2 ng/mL IS solution was added to prepare three sample sets (A, B, and C). Sample set A comprised standard and IS mixed solutions without a cellular matrix. Sample set B comprised the standard solution

and the cellular matrix. Sample set C comprised only the cellular matrix. All sample sets were analyzed, and the peak areas of the analytes and the IS were integrated. The absolute recovery, MF (%), is the combined result of the system recovery rate and matrix effect. The calculated IS-normalized MF is the ratio of the MF to the IS, and was used to evaluate the effect of the measurement method matrix.

$$\text{Matrix factor (\%)} = \frac{(\text{peak area of sample set B} - \text{peak area of sample set C})}{(\text{peak area of sample set A})} \times 100$$

$$\text{IS normalized matrix factor (\%)} = \frac{(\text{matrix factor of analytes})}{(\text{matrix factor of IS})} \times 100$$

3.9. Calibration Curve Preparation

The standard solution was mixed and diluted to 1, 3, 6, 10, 30, 60, 100, 300, and 600 pg/mL, and 1, 3, 6, 10, 30, 60, and 100 ng/mL. After drying 100 μL of the standard solution under a light stream of nitrogen, water (0.5 mL) was added as an alternative matrix, and 1 mL IS solution in AcOEt was added and re-dissolved. The solution was centrifuged at 14,000 rpm for 5 min and the separated upper layer was recovered. Thereafter, 1 mL AcOEt was added to the lower layer, and the centrifugation step was repeated. The upper layers obtained were combined and dried under a nitrogen stream. The standards were re-dissolved in 100 μL water/methanol (1:1, *v/v*) and subjected to both positive and negative mode LC–MS/MS analysis (50 μL per analysis). The peak area ratio of the measurement target and IS was plotted at each concentration and a calibration curve was constructed using the least-squares method with $1/x^2$ weighting.

3.10. Reproducibility Test

QC standard solutions of steroid hormones were dried under a nitrogen stream. Subsequent to the addition of 0.5 mL medium or cells in PBS, 1 mL AcOEt, and 1 mL IS solution in AcOEt, the solution was centrifuged at 14,000 rpm for 5 min to extract the upper layer. Thereafter, 2 mL of AcOEt was added to the lower layer, the centrifugation step was repeated, and the upper layer was re-extracted. The two obtained upper layers were combined, dried under a nitrogen stream, and re-dissolved in 100 μL of 50% methanol. Lastly, 50 μL of each prepared solution was injected for reproducibility measurements.

Three QC standard solutions were prepared for positive (10 compounds) and negative (3 compounds) ion detection mode as LQC (0.3 ng/mL and 0.03 ng/mL, respectively), MQC (3 ng/mL and 0.3 ng/mL, respectively), and HQC (80 ng/mL for both modes).

These QC samples were analyzed using a calibration curve in the same analysis batch (each concentration, *n* = 3). The QC concentration and formula used were as follows:

$$\text{RE (\%)} = \frac{(\text{mean value of each QC value} - [\text{QC concentration} + \text{endougenous concentration})}{(\text{QC concentration} + \text{endogenous concentration})}$$

$$\text{CV (\%)} = \frac{\text{standard deviation of quantitative value}}{\text{mean value of quantitative value}} \times 100$$

3.11. NPC Model Cell and Medium

We used the *Npc1* gene to trap CHO cells as NPC model cells [44], while wild-type CHO cells were used as controls. Dulbecco's modified Eagle's medium (DMEM)/Ham F-12 medium (L-glutamine, pyruvic acid, HEPES-free, phenol red-free) was purchased from Nacalai Tesque and subcultured with deactivated 10% FBS.

3.12. Cholesterol Staining

The filipin staining solution was prepared by mixing filipin (0.5 mg), dimethyl sulfoxide (25 μL), and 10% FBS-supplemented PBS. The cells (2.0×10^5 cells/well) were seeded in 12-well plates on a cover glass. After reaching 90% confluence, the medium was removed,

and the plates were washed with ice-cold PBS before being incubated with 200 μL of 4% paraformaldehyde at 25 °C for 20 min. After washing three times with ice-cold PBS, the plates were incubated with 600 μL of filipin staining solution at 25 °C for 30 min. The plates were washed again twice with ice-cold PBS, and 250 μL PBS was added. The cover glass was then removed, placed on a glass slide, and fixed using an adhesive. Slides were placed under a BZ9000 fluorescence microscope (Keyence, Osaka, Japan), and the cellular unesterified cholesterol was observed using DAPI-BP as a fluorescence filter.

3.13. Organelle Observation

Cover glasses were laid on 12-well plates for cell culture and washed twice with 1 mL ethanol and medium. Thereafter, 2.0×10^5 cells were seeded per well and grown to 90% confluence. The nuclei, lysosomes, and mitochondria were simultaneously stained using Organelle-ID-RGB® reagent I. The staining solution was prepared by diluting 2 μL of the staining reagent with 1 mL PBS. Before staining, the medium was removed, 250 μL of staining solution was added, and the cells were incubated at 37 °C for 30 min. After removal of the staining solution, the cells were washed twice with 250 μL of PBS, and 250 μL of PBS was added. The cover glass was removed, placed on a glass slide, and fixed using an adhesive. Cell and organelle morphology were observed using a BZ9000 fluorescence microscope under a 100-fold oil-immersed objective lens. DAPI-BP (excitation [Ex], 360 nm; emission [Em], 460 nm), GFP-BP (excitation, 470 nm; emission, 535 nm), and TRITC (excitation, 540 nm; emission, 605 nm) were used as fluorescence filters. The shapes of nuclei, mitochondria, and lysosomes were also observed.

3.14. Cells for LC–MS/MS Analysis of Steroid Hormones

The cells (2.0×10^6) were seeded in a 100 mm petri dish and grown in a medium containing 10% FBS. After 24 h, the medium was replaced with FBS-free medium, and the cells were collected after another 48 h. After collecting the medium, the cells were washed twice with 2 mL ice-cold PBS and were subsequently collected from the petri dish using a scraper. Lastly, the suspended cells were counted and analyzed using LC–MS/MS.

3.15. Sample Preparation Procedure

To 2 mL cell suspension containing either 8.6×10^6 cells or 2 mL cell-culturing medium, 1 mL AcOEt and 3 mL IS solution in AcOEt were added, and the suspension was then centrifuged at 3000 rpm for 10 min to separate the upper layer. After fractionation of the upper layer, 4 mL of AcOEt was added to the lower layer, and liquid–liquid extraction was repeated. The two upper layers were combined, dried under nitrogen gas, and redissolved in 100 μL of 50% methanol. Each 50 μL aliquot was subjected to LC–MS/MS analysis for each polarity.

3.16. Quantification of Steroid Hormones in the Sample

Steroid hormones in the cells and medium were analyzed using LC–MS/MS. The peak area of the SRM chromatogram was integrated and quantified using the peak area ratio of each compound relative to the IS.

The amount of steroid hormone in the cell suspension was calculated using the following formula:

$$\text{Amount in cell } (\text{pg}/10^6 \text{ cells})$$
$$= \left(\text{quantified steroid hormones in cell suspension } [\text{pg/mL}] \times \frac{\text{cell suspension volume } [\text{mL}]}{\text{cell count } [10^6 \text{ cells}]} \right)$$

The difference between steroid hormones in the cell cultures were calculated using the following equation:

$$\begin{aligned}
\text{The difference in medium } \left(\text{pg}/10^6 \text{ cells}\right) \\
= \big\{ (\text{quantified steroid hormone in cell culture medium } [\text{pg}/\text{mL}] \\
- \text{quantified steroid hormone in fresh medium } [\text{pg}/\text{mL}]) \times \tfrac{\text{medium volume (mL)}}{\text{cell count } (10^6 \text{ cells})} \big\}
\end{aligned} \tag{1}$$

3.17. Statistical Analysis

All experimental results are presented as mean $\pm$ standard deviation (S.D.). To determine statistically significant differences, a Wilcoxon's test was applied. Differences with * $p < 0.05$ and ** $p < 0.005$ were considered statistically significant.

4. Conclusions

In this study, we developed a method for the simultaneous analysis of steroid hormones using LC–MS/MS to evaluate the associated metabolic changes in NPC model cells, thereby allowing for partial deciphering of the NPC pathophysiology. Following evaluation of LC–MS/MS conditions, pretreatment, and analytical method validation, we succeeded in the simultaneous LC–MS/MS analysis of 13 steroid hormones in cells and media. The levels of steroid hormones, such as androgens and estrogens, were decreased in NPC model cells, possibly due to various impaired mitochondrial functions, suggesting an altered steroid hormone metabolism in NPC patients. As such, the current study has illuminated novel aspects of the NPC pathophysiology, which may be used for the discovery of novel NPC treatment targets in future studies.

Supplementary Materials: The following supporting information can be downloaded at: https://www.mdpi.com/article/10.3390/ijms23084459/s1.

Author Contributions: Conceptualization, M.M. and N.M.; analytical method development and experimental determination, A.A. and M.M.; verification of the properties and morphology of cells, A.A., J.O. and M.M.; cellular experiments, A.A., T.S., Y.S., M.K. (Masaki Kumondai), H.T. and J.O.; formal statistical analysis, M.M.; preparation of cells, K.H.; writing—original draft preparation, A.A. and M.M.; writing—review and editing, A.A., T.S., Y.S., M.K. (Masaki Kumondai), M.K. (Masafumi Kikuchi), K.H. and J.O.; visualization, M.M.; supervision, M.M. and N.M.; project administration, M.M.; funding acquisition, M.M. All authors have read and agreed to the published version of the manuscript.

Institutional Review Board Statement: Not applicable.

Informed Consent Statement: Not applicable.

Data Availability Statement: Not applicable.

Conflicts of Interest: The authors declare no conflict of interest.

References

1. Vanier, M.T. Niemann-Pick Disease Type C. *Orphanet J. Rare Dis.* **2010**, *5*, 16. [CrossRef] [PubMed]
2. Carstea, E.D.; Morris, J.A.; Coleman, K.G.; Loftus, S.K.; Zhang, D.; Cummings, C.; Gu, J.; Rosenfeld, M.A.; Pavan, W.J.; Krizman, D.B.; et al. Niemann-Pick C1 Disease Gene: Homology to Mediators of Cholesterol Homeostasis. *Science* **1997**, *277*, 228–231. [CrossRef] [PubMed]
3. Carstea, E.D.; Polymeropoulos, M.H.; Parker, C.C.; Detera-Wadleigh, S.D.; O'Neill, R.R.; Patterson, M.C.; Goldin, E.; Xiao, H.; Straub, R.E.; Vanier, M.T. Linkage of Niemann-Pick Disease Type C to Human Chromosome 18. *Proc. Natl. Acad. Sci. USA* **1993**, *90*, 2002–2004. [CrossRef] [PubMed]
4. Steinberg, S.J.; Ward, C.P.; Fensom, A.H. Complementation Studies in Niemann-Pick Disease Type C Indicate the Existence of a Second Group. *J. Med. Genet.* **1994**, *31*, 317–320. [CrossRef] [PubMed]
5. Naureckiene, S.; Sleat, D.E.; Lackland, H.; Fensom, A.; Vanier, M.T.; Wattiaux, R.; Jadot, M.; Lobel, P. Identification of HE1 as the Second Gene of Niemann-Pick C Disease. *Science* **2000**, *290*, 2298–2301. [CrossRef]

6. Kwon, H.J.; Abi-Mosleh, L.; Wang, M.L.; Deisenhofer, J.; Goldstein, J.L.; Brown, M.S.; Infante, R.E. Structure of N-Terminal Domain of NPC1 Reveals Distinct Subdomains for Binding and Transfer of Cholesterol. *Cell* **2009**, *137*, 1213–1224. [CrossRef]

7. Patterson, M.C.; Hendriksz, C.J.; Walterfang, M.; Sedel, F.; Vanier, M.T.; Wijburg, F. Recommendations for the Diagnosis and Management of Niemann-Pick Disease Type C: An Update. *Mol. Genet. Metab.* **2012**, *106*, 330–344. [CrossRef]

8. Patterson, M.C.; Clayton, P.; Gissen, P.; Anheim, M.; Bauer, P.; Bonnot, O.; Dardis, A.; Dionisi-Vici, C.; Klünemann, H.H.; Latour, P.; et al. Recommendations for the Detection and Diagnosis of Niemann-Pick Disease Type C: An Update. *Neurol. Clin. Pract.* **2017**, *7*, 499–511. [CrossRef]

9. Geberhiwot, T.; Moro, A.; Dardis, A.; Ramaswami, U.; Sirrs, S.; Marfa, M.P.; Vanier, M.T.; Walterfang, M.; Bolton, S.; Dawson, C.; et al. Consensus Clinical Management Guidelines for Niemann-Pick Disease Type C. *Orphanet J. Rare Dis.* **2018**, *13*, 50. [CrossRef]

10. Patterson, M. *Niemann-Pick Disease Type C*; University of Washington: Seattle, WA, USA, 1993.

11. Ohno, K. Niemann-Pick Type C Disease: Pathophysiology, Diagnosis and Treatment. *No Hattatsu* **2016**, *48*, 81–88. [CrossRef]

12. Patterson, M.C.; Mengel, E.; Vanier, M.T.; Schwierin, B.; Muller, A.; Cornelisse, P.; Pineda, M.; Amado-Fondo, A.; Amraoui, Y.; Andria, G.; et al. Stable or Improved Neurological Manifestations during Miglustat Therapy in Patients from the International Disease Registry for Niemann-Pick Disease Type C: An Observational Cohort Study. *Orphanet J. Rare Dis.* **2015**, *10*, 65. [CrossRef] [PubMed]

13. Ory, D.S.; Ottinger, E.A.; Farhat, N.Y.; King, K.A.; Jiang, X.; Weissfeld, L.; Berry-Kravis, E.; Davidson, C.D.; Bianconi, S.; Keener, L.A.; et al. Intrathecal 2-Hydroxypropyl-β-Cyclodextrin Decreases Neurological Disease Progression in Niemann-Pick Disease, Type C1: A Non-Randomised, Open-Label, Phase 1–2 Trial. *Lancet* **2017**, *390*, 1758–1768. [CrossRef]

14. Shioi, R.; Karaki, F.; Yoshioka, H.; Noguchi-Yachide, T.; Ishikawa, M.; Dodo, K.; Hashimoto, Y.; Sodeoka, M.; Ohgane, K. Image-Based Screen Capturing Misfolding Status of Niemann-Pick Type C1 Identifies Potential Candidates for Chaperone Drugs. *PLoS ONE* **2020**, *15*, e0243746. [CrossRef] [PubMed]

15. Pipalia, N.H.; Saad, S.Z.; Subramanian, K.; Cross, A.; al-Motawa, A.; Garg, K.; Blagg, B.S.J.; Neckers, L.; Helquist, P.; Wiest, O.; et al. HSP90 Inhibitors Reduce Cholesterol Storage in Niemann-Pick Type C1 Mutant Fibroblasts. *J. Lipid Res.* **2021**, *63*, 100114. [CrossRef]

16. Kirkegaard, T.; Roth, A.G.; Petersen, N.H.T.; Mahalka, A.K.; Olsen, O.D.; Moilanen, I.; Zylicz, A.; Knudsen, J.; Sandhoff, K.; Arenz, C.; et al. Hsp70 Stabilizes Lysosomes and Reverts Niemann-Pick Disease-Associated Lysosomal Pathology. *Nature* **2010**, *463*, 549–553. [CrossRef]

17. Fukuda, H.; Karaki, F.; Dodo, K.; Noguchi-Yachide, T.; Ishikawa, M.; Hashimoto, Y.; Ohgane, K. Phenanthridin-6-One Derivatives as the First Class of Non-Steroidal Pharmacological Chaperones for Niemann-Pick Disease Type C1 Protein. *Bioorg. Med. Chem. Lett.* **2017**, *27*, 2781–2787. [CrossRef]

18. Paulina Ordonez, M.; Roberts, E.A.; Kidwell, C.U.; Yuan, S.H.; Plaisted, W.C.; Goldstein, L.S.B. Disruption and Therapeutic Rescue of Autophagy in a Human Neuronal Model of Niemann Pick Type C1. *Hum. Mol. Genet.* **2012**, *21*, 2651–2662. [CrossRef]

19. Elrick, M.J.; Yu, T.; Chung, C.; Lieberman, A.P. Impaired Proteolysis Underlies Autophagic Dysfunction in Niemann-Pick Type C Disease. *Hum. Mol. Genet.* **2012**, *21*, 4876–4887. [CrossRef]

20. Ordonez, M.P. Defective Mitophagy in Human Niemann-Pick Type C1 Neurons Is Due to Abnormal Autophagy Activation. *Autophagy* **2012**, *8*, 1157–1158. [CrossRef]

21. Guo, H.; Zhao, M.; Qiu, X.; Deis, J.A.; Huang, H.; Tang, Q.Q.; Chen, X. Niemann-Pick Type C2 Deficiency Impairs Autophagylyso-somal Activity, Mitochondrial Function, and TLR Signaling in Adipocytes. *J. Lipid Res.* **2016**, *57*, 1644–1658. [CrossRef]

22. Torres, S.; Balboa, E.; Zanlungo, S.; Enrich, C.; Garcia-Ruiz, C.; Fernandez-Checa, J.C. Lysosomal and Mitochondrial Liaisons in Niemann-Pick Disease. *Front. Physiol.* **2017**, *8*, 982. [CrossRef]

23. Yu, W.; Gong, J.S.; Ko, M.; Garver, W.S.; Yanagisawa, K.; Michikawa, M. Altered Cholesterol Metabolism in Niemann-Pick Type C1 Mouse Brains Affects Mitochondrial Function. *J. Biol. Chem.* **2005**, *280*, 11731–11739. [CrossRef] [PubMed]

24. Torres, S.; Matías, N.; Baulies, A.; Nuñez, S.; Alarcon-Vila, C.; Martinez, L.; Nuño, N.; Fernandez, A.; Caballeria, J.; Levade, T.; et al. Mitochondrial GSH Replenishment as a Potential Therapeutic Approach for Niemann Pick Type C Disease. *Redox Biol.* **2017**, *11*, 60–72. [CrossRef] [PubMed]

25. Payne, A.H.; Hales, D.B. Overview of Steroidogenic Enzymes in the Pathway from Cholesterol to Active Steroid Hormones. *Endocr. Rev.* **2004**, *25*, 947–970. [CrossRef] [PubMed]

26. Miller, W.L. Steroid Hormone Synthesis in Mitochondria. *Mol. Cell. Endocrinol.* **2013**, *379*, 62–73. [CrossRef]

27. Miller, W.L.; Auchus, R.J. The Molecular Biology, Biochemistry, and Physiology of Human Steroidogenesis and Its Disorders. *Endocr. Rev.* **2011**, *32*, 81–151. [CrossRef]

28. Cole, T.J.; Short, K.L.; Hooper, S.B. The Science of Steroids. *Semin. Fetal Neonatal Med.* **2019**, *24*, 170–175. [CrossRef]

29. Holst, J.P.; Soldin, O.P.; Guo, T.; Soldin, S.J. Steroid Hormones: Relevance and Measurement in the Clinical Laboratory. *Clin. Lab. Med.* **2004**, *24*, 105–118. [CrossRef]

30. Gévry, N.Y.; Lopes, F.L.; Ledoux, S.; Murphy, B.D. Aberrant Intracellular Cholesterol Transport Disrupts Pituitary and Ovarian Function. *Mol. Endocrinol.* **2004**, *18*, 1778–1786. [CrossRef]

31. Chen, G.; Li, H.M.; Chen, Y.R.; Gu, X.S.; Duan, S. Decreased Estradiol Release from Astrocytes Contributes to the Neurodegeneration in a Mouse Model of Niemann-Pick Disease Type C. *GLIA* **2007**, *55*, 1509–1518. [CrossRef]

32. Xie, C.; Richardson, J.A.; Turley, S.D.; Dietschy, J.M. Cholesterol Substrate Pools and Steroid Hormone Levels Are Normal in the Face of Mutational Inactivation of NPC1 Protein. *J. Lipid Res.* **2006**, *47*, 953–963. [CrossRef] [PubMed]

33. Griffin, L.D.; Gong, W.; Verot, L.; Mellon, S.H. Niemann-Pick Type C Disease Involves Disrupted Neurosteroidogenesis and Responds to Allopregnanolone. *Nat. Med.* **2004**, *10*, 704–711. [CrossRef] [PubMed]

34. Akpovi, C.D.; Murphy, B.D.; Erickson, R.P.; Pelletier, R.-M. Dysregulation of Testicular Cholesterol Metabolism Following Spontaneous Mutation of the Niemann-Pick C1 Gene in Mice1. *Biol. Reprod.* **2014**, *91*, 42–43. [CrossRef] [PubMed]

35. Mellon, S.H.; Gong, W.; Schonemann, M.D. Endogenous and Synthetic Neurosteroids in Treatment of Niemann-Pick Type C Disease. *Brain Res. Rev.* **2008**, *57*, 410–420. [CrossRef] [PubMed]

36. Miller, W.L. Disorders in the Initial Steps of Steroid Hormone Synthesis. *J. Steroid Biochem. Mol. Biol.* **2017**, *165*, 18–37. [CrossRef]

37. Lamri, A.; Pigeyre, M.; Garver, W.S.; Meyre, D. The Extending Spectrum of NPC1-Related Human Disorders: From Niemann–Pick C1 Disease to Obesity. *Endocr. Rev.* **2018**, *39*, 192–220. [CrossRef]

38. Barnard, G.; Kohen, F. Monitoring Ovarian Function by the Simultaneous Time-Resolved Fluorescence Immunoassay of Two Urinary Steroid Metabolites. *Clin. Chem.* **1998**, *44*, 1520–1528. [CrossRef]

39. Keevil, B.G. LC–MS/MS Analysis of Steroids in the Clinical Laboratory. *Clin. Biochem.* **2016**, *49*, 989–997. [CrossRef]

40. Higashi, T.; Shimada, K. Derivatization of Neutral Steroids to Enhance Their Detection Characteristics in Liquid Chromatography-Mass Spectrometry. *Anal. Bioanal. Chem.* **2004**, *378*, 875–882. [CrossRef]

41. Higashi, T.; Ogawa, S. Chemical Derivatization for Enhancing Sensitivity during LC/ESI–MS/MS Quantification of Steroids in Biological Samples: A Review. *J. Steroid Biochem. Mol. Biol.* **2016**, *162*, 57–69. [CrossRef]

42. Higaki, K.; Ninomiya, H.; Sugimoto, Y.; Suzuki, T.; Taniguchi, M.; Niwa, H.; Pentchev, P.G.; Vanier, M.T.; Ohno, K. Isolation of NPC1-Deficient Chinese Hamster Ovary Cell Mutants by Gene Trap Mutagenesis. *J. Biochem.* **2001**, *129*, 875–880. [CrossRef] [PubMed]

43. Keski-Rahkonen, P.; Desai, R.; Jimenez, M.; Harwood, D.T.; Handelsman, D.J. Measurement of Estradiol in Human Serum by LC-MS/MS Using a Novel Estrogen-Specific Derivatization Reagent. *Anal. Chem.* **2015**, *87*, 7180–7186. [CrossRef] [PubMed]

44. Higashi, T.; Shimada, K. Application of Cookson-Type Reagents for Biomedical HPLC and LC/MS Analyses: A Brief Overview. *Biomed. Chromatogr.* **2017**, *31*, e3808. [CrossRef] [PubMed]

45. Lavrynenko, O.; Nedielkov, R.; Möller, H.M.; Shevchenko, A. Girard Derivatization for LC-MS/MS Profiling of Endogenous Ecdysteroids in Drosophila. *J. Lipid Res.* **2013**, *54*, 2265–2272. [CrossRef] [PubMed]

46. Higashi, T.; Ogawa, S. Isotope-Coded ESI-Enhancing Derivatization Reagents for Differential Analysis, Quantification and Profiling of Metabolites in Biological Samples by LC/MS: A Review. *J. Pharm. Biomed. Anal.* **2016**, *130*, 181–193. [CrossRef]

47. Yuan, T.F.; Le, J.; Cui, Y.; Peng, R.; Wang, S.T.; Li, Y. An LC-MS/MS Analysis for Seven Sex Hormones in Serum. *J. Pharm. Biomed. Anal.* **2019**, *162*, 34–40. [CrossRef]

48. Yuan, T.F.; Le, J.; Wang, S.T.; Li, Y. An LC/MS/MS Method for Analyzing the Steroid Metabolome with High Accuracy and from Small Serum Samples. *J. Lipid Res.* **2020**, *61*, 580–586. [CrossRef]

49. Li, X.; Li, S.; Kellermann, G. Simultaneous Determination of Three Estrogens in Human Saliva without Derivatization or Liquid-Liquid Extraction for Routine Testing via Miniaturized Solid Phase Extraction with LC-MS/MS Detection. *Talanta* **2018**, *178*, 464–472. [CrossRef]

50. Márta, Z.; Bobály, B.; Fekete, J.; Magda, B.; Imre, T.; Mészáros, K.V.; Bálint, M.; Szabó, P.T. Simultaneous Determination of Thirteen Different Steroid Hormones Using Micro UHPLC-MS/MS with on-Line SPE System. *J. Pharm. Biomed. Anal.* **2018**, *150*, 258–267. [CrossRef]

51. Gaudl, A.; Kratzsch, J.; Bae, Y.J.; Kiess, W.; Thiery, J.; Ceglarek, U. Liquid Chromatography Quadrupole Linear Ion Trap Mass Spectrometry for Quantitative Steroid Hormone Analysis in Plasma, Urine, Saliva and Hair. *J. Chromatogr. A* **2016**, *1464*, 64–71. [CrossRef]

52. Tan, A.; Wu, Y.; Wong, M.; Licollari, A.; Bolger, G.; Fanaras, J.C.; Shopp, G.; Helson, L. Use of Basic Mobile Phase to Improve Chromatography and Boost Sensitivity for Quantifying Tetrahydrocurcumin in Human Plasma by LC-MS/MS. *J. Chromatogr. B Anal. Technol. Biomed. Life Sci.* **2016**, *1028*, 86–93. [CrossRef] [PubMed]

53. Tan, A.; Gu, G.; Gui, X.; Wu, Y.; Bolger, G.; Licollari, A.; Fanaras, J.C. Improving the Selectivity and Sensitivity for Quantifying 8-α-Hydroxy-Mutilin in Rabbit Tissues by Using Basic Mobile Phases and Negative Ionization. *J. Chromatogr. B Anal. Technol. Biomed. Life Sci.* **2018**, *1072*, 142–148. [CrossRef] [PubMed]

54. Nakano, Y.; Nagasawa, E.; Uchida, T.; Sakamaki, H. Highly Sensitive Detection of Pesticide Residues by LC-MS/MS Using Ammonia Solution as an Eluent. *Bunseki Kagaku* **2020**, *69*, 141–150. [CrossRef]

55. Lewis, K.M.; Archer, R.D. PKa Values of Estrone, 17β-Estradiol and 2-Methoxyestrone. *Steroids* **1979**, *34*, 485–499. [CrossRef]

56. Nouri, M.Z.; Kroll, K.J.; Webb, M.; Denslow, N.D. Quantification of Steroid Hormones in Low Volume Plasma and Tissue Homogenates of Fish Using LC-MS/MS. *Gen. Comp. Endocrinol.* **2020**, *296*, 113543. [CrossRef]

57. Maekawa, M.; Jinnoh, I.; Narita, A.; Iida, T.; Saigusa, D.; Iwahori, A.; Nittono, H.; Okuyama, T.; Eto, Y.; Ohno, K.; et al. Investigation of Diagnostic Performance of Five Urinary Cholesterol Metabolites for Niemann-Pick Disease Type C. *J. Lipid Res.* **2019**, *60*, 2074–2081. [CrossRef]

58. Iwahori, A.; Maekawa, M.; Narita, A.; Kato, A.; Sato, T.; Ogura, J.; Sato, Y.; Kikuchi, M.; Noguchi, A.; Higaki, K.; et al. Development of a Diagnostic Screening Strategy for Niemann–Pick Diseases Based on Simultaneous Liquid Chromatography-Tandem Mass Spectrometry Analyses of N-Palmitoyl-O-Phosphocholine-Serine and Sphingosylphosphorylcholine. *Biol. Pharm. Bull.* **2020**, *43*, 1398–1406. [CrossRef]

59. Maekawa, M.; Misawa, Y.; Sotoura, A.; Yamaguchi, H.; Togawa, M.; Ohno, K.; Nittono, H.; Kakiyama, G.; Iida, T.; Hofmann, A.F.; et al. LC/ESI-MS/MS Analysis of Urinary 3β-Sulfooxy-7β-N-Acetylglucosaminyl-5-Cholen-24-Oic Acid and Its Amides: New Biomarkers for the Detection of Niemann–Pick Type C Disease. *Steroids* **2013**, 78, 967–972. [CrossRef]

60. Maekawa, M.; Narita, A.; Jinnoh, I.; Iida, T.; Marquardt, T.; Mengel, E.; Eto, Y.; Clayton, P.T.; Yamaguchi, H.; Mano, N. Diagnostic Performance Evaluation of Sulfate-Conjugated Cholesterol Metabolites as Urinary Biomarkers of Niemann–Pick Disease Type C. *Clin. Chim. Acta* **2019**, 494, 58–63. [CrossRef]

61. Shoji, S.; Maekawa, M.; Ogura, J.; Sato, T.; Mano, N. Identification Cholesterol Metabolites Altered before the Onset of Nonalcoholic Steatohepatitis by Targeted Metabolomics. *Biochim. Biophys. Acta (BBA)—Mol. Cell Biol. Lipids* **2022**, 1867, 159135. [CrossRef]

62. Welford, R.W.D.; Garzotti, M.; Marques Lourenço, C.; Mengel, E.; Marquardt, T.; Reunert, J.; Amraoui, Y.; Kolb, S.A.; Morand, O.; Groenen, P. Plasma Lysosphingomyelin Demonstrates Great Potential as a Diagnostic Biomarker for Niemann-Pick Disease Type C in a Retrospective Study. *PLoS ONE* **2014**, 9, e114669. [CrossRef] [PubMed]

63. Sobrido, M.J.; Bauer, P.; de Koning, T.; Klopstock, T.; Nadjar, Y.; Patterson, M.C.; Synofzik, M.; Hendriksz, C.J. Recommendations for Patient Screening in Ultra-Rare Inherited Metabolic Diseases: What Have We Learned from Niemann-Pick Disease Type C? *Orphanet J. Rare Dis.* **2019**, 14, 20. [CrossRef]

64. Feng, X.; Cozma, C.; Pantoom, S.; Hund, C.; Iwanov, K.; Petters, J.; Völkner, C.; Bauer, C.; Vogel, F.; Bauer, P.; et al. Determination of the Pathological Features of NPC1 Variants in a Cellular Complementation Test. *Int. J. Mol. Sci.* **2019**, 20, 5185. [CrossRef] [PubMed]

65. Pentchev, P.G.; Boothe, A.D.; Kurth, H.S. A Genetic Storage Disorder in BALB/C Mice with a Metabolic Block in Esterification of Exogenous Cholesterol. *J. Biol. Chem.* **1984**, 259, 5784–5791. [CrossRef]

66. Tint, G.S.; Pentchev, P.; Xu, G.; Batta, A.K.; Shefer, S.; Salen, G.; Honda, A. Cholesterol and Oxygenated Cholesterol Concentrations Are Markedly Elevated in Peripheral Tissue but Not in Brain from Mice with the Niemann-Pick Type C Phenotype. *J. Inherit. Metab. Dis.* **1998**, 21, 853–863. [CrossRef]

67. Pentchev, P.G.; Comly, M.E.; Kruth, H.S.; Vanier, M.T.; Wenger, D.A.; Patel, S.; Brady, R.O. A Defect in Cholesterol Esterification in Niemann-Pick Disease (Type C) Patients. *Proc. Natl. Acad. Sci. USA* **1985**, 82, 8247–8251. [CrossRef]

68. Vanier, M.T.; Latour, P. Laboratory Diagnosis of Niemann-Pick Disease Type C: The Filipin Staining Test. *Methods Cell Biol.* **2015**, 126, 357–375. [CrossRef]

69. Liedtke, M.; Völkner, C.; Hermann, A.; Frech, M.J. Impact of Organelle Transport Deficits on Mitophagy and Autophagy in Niemann–Pick Disease Type C. *Cells* **2022**, 11, 507. [CrossRef]

70. Davis, O.B.; Shin, H.R.; Lim, C.Y.; Wu, E.Y.; Kukurugya, M.; Maher, C.F.; Perera, R.M.; Ordonez, M.P.; Zoncu, R. NPC1-MTORC1 Signaling Couples Cholesterol Sensing to Organelle Homeostasis and Is a Targetable Pathway in Niemann-Pick Type C. *Dev. Cell* **2021**, 56, 260–276.e7. [CrossRef]

71. Hecker, M.; Hollert, H.; Cooper, R.; Vinggaard, A.M.; Akahori, Y.; Murphy, M.; Nellemann, C.; Higley, E.; Newsted, J.; Laskey, J.; et al. The OECD Validation Program of the H295R Steroidogenesis Assay: Phase 3. Final Inter-Laboratory Validation Study. *Environ. Sci. Pollut. Res.* **2011**, 18, 503–515. [CrossRef]

72. Weisser, J.J.; Hansen, C.H.; Poulsen, R.; Larsen, L.W.; Cornett, C.; Styrishave, B. Two Simple Cleanup Methods Combined with LC-MS/MS for Quantification of Steroid Hormones in In Vivo and In Vitro Assays. *Anal. Bioanal. Chem.* **2016**, 408, 4883–4895. [CrossRef] [PubMed]

73. Kumar, N.; Srivastava, S.; Burek, M.; Förster, C.Y.; Roy, P. Assessment of Estradiol-Induced Gene Regulation and Proliferation in an Immortalized Mouse Immature Sertoli Cell Line. *Life Sci.* **2016**, 148, 268–278. [CrossRef] [PubMed]

74. Berthois, Y.; Katzenellenbogen, J.A.; Katzenellenbogen, B.S. Phenol Red in Tissue Culture Media Is a Weak Estrogen: Implications Concerning the Study of Estrogen-Responsive Cells in Culture. *Proc. Natl. Acad. Sci. USA* **1986**, 83, 2496–2500. [CrossRef] [PubMed]

75. Strajhar, P.; Tonoli, D.; Jeanneret, F.; Imhof, R.M.; Malagnino, V.; Patt, M.; Kratschmar, D.v.; Boccard, J.; Rudaz, S.; Odermatt, A. Steroid Profiling in H295R Cells to Identify Chemicals Potentially Disrupting the Production of Adrenal Steroids. *Toxicology* **2017**, 381, 51–63. [CrossRef] [PubMed]

76. Jee, J.P.; Jin, S.E.; Ban, E.; Lee, H.J.; Park, Y.; Park, Y.; Maeng, H.J.; Kim, H.T.; Kim, C.K. Isolation and Identification of Steroidogenic Peptides from Calf Spleen. *Arch. Pharm. Res.* **2012**, 35, 653–658. [CrossRef] [PubMed]

77. Ahmed, K.E.M.; Frøysa, H.G.; Karlsen, O.A.; Sagen, J.v.; Mellgren, G.; Verhaegen, S.; Ropstad, E.; Goksøyr, A.; Kellmann, R. LC-MS/MS Based Profiling and Dynamic Modelling of the Steroidogenesis Pathway in Adrenocarcinoma H295R Cells. *Toxicol. Vitr.* **2018**, 52, 332–341. [CrossRef] [PubMed]

78. Kurlbaum, M.; Sbiera, S.; Kendl, S.; Martin Fassnacht, M.; Kroiss, M. Steroidogenesis in the NCI-H295 Cell Line Model Is Strongly Affected by Culture Conditions and Substrain. *Exp. Clin. Endocrinol. Diabetes* **2020**, 128, 672–680. [CrossRef]

79. Winther, C.S.; Nielsen, F.K.; Hansen, M.; Styrishave, B. Corticosteroid Production in H295R Cells during Exposure to 3 Endocrine Disrupters Analyzed with LC-MS/MS. *Int. J. Toxicol.* **2013**, 32, 219–227. [CrossRef]

80. Munkboel, C.H.; Baake, M.L.K.; Styrishave, B. Atorvastatin Decreases Steroid Production in H295R Cells and in Major Endocrine Tissues of Male Rats. *Arch. Toxicol.* **2018**, 92, 1703–1715. [CrossRef]

81. Machioka, K.; Mizokami, A.; Yamaguchi, Y.; Izumi, K.; Hayashi, S.; Namiki, M. Active Estrogen Synthesis and Its Function in Prostate Cancer-Derived Stromal Cells. *Anticancer Res.* **2015**, 35, 221–228.

82. Hansen, C.H.; Larsen, L.W.; Sørensen, A.M.; Halling-Sørensen, B.; Styrishave, B. The Six Most Widely Used Selective Serotonin Reuptake Inhibitors Decrease Androgens and Increase Estrogens in the H295R Cell Line. *Toxicol. In Vitro* **2017**, *41*, 1–11. [CrossRef] [PubMed]

83. Blaschke, M.; Koepp, R.; Streit, F.; Beismann, J.; Manthey, G.; Seitz, M.T.; Kragl, A.; Siggelkow, H. The Rise in Expression and Activity of 11β-HSD1 in Human Mesenchymal Progenitor Cells Induces Adipogenesis through Increased Local Cortisol Synthesis. *J. Steroid Biochem. Mol. Biol.* **2021**, *210*, 105850. [CrossRef] [PubMed]

84. Fujiki, J.; Maeda, N.; Sato, M.; Ieko, T.; Inoue, H.; Iwasaki, T.; Iwano, H.; Yokota, H. Corticosterone Biosynthesis in Mouse Clonal Myoblastic C2C12 Cells. *Steroids* **2018**, *138*, 64–71. [CrossRef] [PubMed]

85. Koal, T.; Schmiederer, D.; Pham-Tuan, H.; Röhring, C.; Rauh, M. Standardized LC-MS/MS Based Steroid Hormone Profile-Analysis. *J. Steroid Biochem. Mol. Biol.* **2012**, *129*, 129–138. [CrossRef] [PubMed]

86. Chen, F.; Cheng, Z.; Peng, Y.; Wang, Z.; Huang, C.; Liu, D.; Wang, B.; Pan, B.; Guo, W. A Liquid Chromatography-Tandem Mass Spectrometry (LC-MS/MS)-Based Assay for Simultaneous Quantification of Aldosterone, Renin Activity, and Angiotensin II in Human Plasma. *J. Chromatogr. B Anal. Technol. Biomed. Life Sci.* **2021**, *1179*, 122740. [CrossRef] [PubMed]

87. Miller, W.L.; Geller, D.H.; Rosen, M. Ovarian and Adrenal Androgen Biosynthesis and Metabolism. In *Androgen Excess Disorders in Women*; Humana Press: Totowa, NJ, USA, 2007; pp. 19–33.

88. Illingworth, D.R.; Corbin, D.K.; Kemp, E.D.; Keenan, E.J. Hormone Changes during the Menstrual Cycle in Abetalipoproteinemia: Reduced Luteal Phase Progesterone in a Patient with Homozygous Hypobetalipoproteinemia. *Proc. Natl. Acad. Sci. USA* **1982**, *79*, 6685–6689. [CrossRef]

89. Miller, W.L. Steroidogenesis: Unanswered Questions. *Trends Endocrinol. Metab.* **2017**, *28*, 771–793. [CrossRef]

90. Kallen, C.B.; Arakane, F.; Christenson, L.K.; Watari, H.; Devoto, L.; Strauss, J.F. Unveiling the Mechanism of Action and Regulation of the Steroidogenic Acute Regulatory Protein. *Mol. Cell. Endocrinol.* **1998**, *145*, 39–45. [CrossRef]

91. Chien, Y.; Rosal, K.; Chung, B. chu Function of CYP11A1 in the Mitochondria. *Mol. Cell. Endocrinol.* **2017**, *441*, 55–61. [CrossRef]

92. Simard, J.; Ricketts, M.-L.; Gingras, S.; Soucy, P.; Feltus, F.A.; Melner, M.H. Molecular Biology of the 3beta-Hydroxysteroid Dehydrogenase/Delta5-Delta4 Isomerase Gene Family. *Endocr. Rev.* **2005**, *26*, 525–582. [CrossRef]

93. Akhtar, M.; Wright, J.N.; Lee-Robichaud, P. A Review of Mechanistic Studies on Aromatase (CYP19) and 17α-Hydroxylase-17,20-Lyase (CYP17). *J. Steroid Biochem. Mol. Biol.* **2011**, *125*, 2–12. [CrossRef] [PubMed]

94. Klinge, C.M.; Clark, B.J.; Prough, R.A. *Dehydroepiandrosterone Research: Past, Current, and Future*, 1st ed.; Elsevier Inc.: Amsterdam, The Netherlands, 2018; Volume 108, ISBN 9780128143612.

95. Meng, L.; Yu, H.; Qu, J.; Niu, J.; Ni, F.; Han, P.; Wang, X. Two Cyp17 Genes Perform Different Functions in the Sex Hormone Biosynthesis and Gonadal Differentiation in Japanese Flounder (Paralichthys Olivaceus). *Gene* **2019**, *702*, 17–26. [CrossRef] [PubMed]

96. Carmina, E. Ovarian and Adrenal Hyperandrogenism. *Ann. N. Y. Acad. Sci.* **2006**, *1092*, 130–137. [CrossRef] [PubMed]

97. Chatuphonprasert, W.; Jarukamjorn, K.; Ellinger, I. Physiology and Pathophysiology of Steroid Biosynthesis, Transport and Metabolism in the Human Placenta. *Front. Pharmacol.* **2018**, *9*, 1027. [CrossRef]

98. Bulun, S.E.; Yang, S.; Fang, Z.; Gurates, B.; Tamura, M.; Zhou, J.; Sebastian, S. Role of Aromatase in Endometrial Disease. *J. Steroid Biochem. Mol. Biol.* **2001**, *79*, 19–25. [CrossRef]

99. Thomas, M.P.; Potter, B.V.L. The Structural Biology of Oestrogen Metabolism. *J. Steroid Biochem. Mol. Biol.* **2013**, *137*, 27–49. [CrossRef]

100. Walker, M.A.; Tian, R. NAD(H) in Mitochondrial Energy Transduction: Implications for Health and Disease. *Curr. Opin. Physiol.* **2018**, *3*, 101–109. [CrossRef]

101. Allen, J.A.; Shankara, T.; Janus, P.; Buck, S.; Diemer, T.; Hales, K.H.; Hales, D.B. Energized, Polarized, and Actively Respiring Mitochondria Are Required for Acute Leydig Cell Steroidogenesis. *Endocrinology* **2006**, *147*, 3924–3935. [CrossRef]

102. Midzak, A.S.; Chen, H.; Aon, M.A.; Papadopoulos, V.; Zirkin, B.R. ATP Synthesis, Mitochondrial Function, and Steroid Biosynthesis in Rodent Primary and Tumor Leydig Cells 1. *Biol. Reprod.* **2011**, *84*, 976–985. [CrossRef]

103. Romano, S.; Mitro, N.; Giatti, S.; Diviccaro, S.; Pesaresi, M.; Spezzano, R.; Audano, M.; Garcia-Segura, L.M.; Caruso, D.; Melcangi, R.C. Diabetes Induces Mitochondrial Dysfunction and Alters Cholesterol Homeostasis and Neurosteroidogenesis in the Rat Cerebral Cortex. *J. Steroid Biochem. Mol. Biol.* **2018**, *178*, 108–116. [CrossRef]

104. Pesaresi, M.; Maschi, O.; Giatti, S.; Miguel Garcia-Segura, L.; Caruso, D.; Cosimo Melcangi, R. Sex Differences in Neuroactive Steroid Levels in the Nervous System of Diabetic and Non-Diabetic Rats. *Horm. Behav.* **2009**, *57*, 46–55. [CrossRef] [PubMed]

105. Romano, S.; Mitro, N.; Diviccaro, S.; Spezzano, R.; Audano, M.; Garcia-Segura, L.M.; Caruso, D.; Melcangi, R.C. Short-Term Effects of Diabetes on Neurosteroidogenesis in the Rat Hippocampus. *J. Steroid Biochem. Mol. Biol.* **2017**, *167*, 135–143. [CrossRef] [PubMed]

106. Meimaridou, E.; Goldsworthy, M.; Chortis, V.; Fragouli, E.; Foster, P.A.; Arlt, W.; Cox, R.; Metherell, L.A. NNT Is a Key Regulator of Adrenal Redox Homeostasis and Steroidogenesis in Male Mice. *J. Endocrinol.* **2018**, *236*, 13–28. [CrossRef]

107. Mangelsdorf, D.J.; Thummel, C.; Beato, M.; Herrlich, P.; Schütz, G.; Umesono, K.; Blumberg, B.; Kastner, P.; Mark, M.; Chambon, P.; et al. The Nuclear Receptor Superfamily: The Second Decade. *Cell* **1995**, *83*, 835–839. [CrossRef]

108. DeMayo, F.J.; Zhao, B.; Takamoto, N.; Tsai, S.Y. Mechanisms of Action of Estrogen and Progesterone. *Ann. N. Y. Acad. Sci.* **2002**, *955*, 48–59. [CrossRef] [PubMed]

109. Kicman, A.T. Pharmacology of Anabolic Steroids. *Br. J. Pharmacol.* **2008**, *154*, 502–521. [CrossRef]

110. Diaz Brinton, R. The Neurosteroid 3α-Hydroxy-5α-Pregnan-20-One Induces Cytoarchitectural Regression in Cultured Fetal Hippocampal Neurons. *J. Neurosci.* **1994**, *14*, 2763–2774. [CrossRef]

111. Concas, A.; Mostallino, M.C.; Porcu, P.; Follesa, P.; Barbaccia, M.L.; Trabucchi, M.; Purdy, R.H.; Grisenti, P.; Biggio, G. Role of Brain Allopregnanolone in the Plasticity of γ-Aminobutyric Acid Type A Receptor in Rat Brain during Pregnancy and after Delivery. *Proc. Natl. Acad. Sci. USA* **1998**, *95*, 13284–13289. [CrossRef]

112. Brussaard, A.B.; Wossink, J.; Lodder, J.C.; Kits, K.S. Progesterone-Metabolite Prevents Protein Kinase c-Dependent Modulation of γ-Aminobutyric Acid Type A Receptors in Oxytocin Neurons. *Proc. Natl. Acad. Sci. USA* **2000**, *97*, 3625–3630. [CrossRef]

113. Reddy, D.S. Neurosteroids. Endogenous Role in the Human Brain and Therapeutic Potentials. In *Progress in Brain Research*; Elsevier B.V.: Amsterdam, The Netherlands, 2010; Volume 186, pp. 113–137.

114. Tsutsui, K.; Ukena, K.; Sakamoto, H.; Okuyama, S.I.; Haraguchi, S. Biosynthesis, Mode of Action, and Functional Significance of Neurosteroids in the Purkinje Cell. *Front. Endocrinol.* **2011**, *2*, 61. [CrossRef]

115. Ko, D.C.; Milenkovic, L.; Beier, S.M.; Manuel, H.; Buchanan, J.A.; Scott, M.P. Cell-Autonomous Death of Cerebellar Purkinje Neurons with Autophagy in Niemann-Pick Type C Disease. *PLoS Genet.* **2005**, *1*, e7. [CrossRef]

116. Kawazoe, T.; Yamamoto, T.; Narita, A.; Ohno, K.; Adachi, K.; Nanba, E.; Noguchi, A.; Takahashi, T.; Maekawa, M.; Eto, Y.; et al. Phenotypic Variability of Niemann-Pick Disease Type C Including a Case with Clinically Pure Schizophrenia: A Case Report. *BMC Neurol.* **2018**, *18*, 117. [CrossRef] [PubMed]

117. Maekawa, M.; Jinnoh, I.; Matsumoto, Y.; Narita, A.; Mashima, R.; Takahashi, H.; Iwahori, A.; Saigusa, D.; Fujii, K.; Abe, A.; et al. Structural Determination of Lysosphingomyelin-509 and Discovery of Novel Class Lipids from Patients with Niemann-Pick Disease Type C. *Int. J. Mol. Sci.* **2019**, *20*, 5018. [CrossRef] [PubMed]